J. Fluid Mech. (2012), *vol.* 690, *pp.* 499–511.
doi:10.1017/jfm.2011.454

Grainsize dynamics of polydisperse granular segregation down inclined planes

Benjy Marks, Pierre Rognon and Itai Einav†

Particles and Grains Laboratory, School of Civil Engineering, The University of Sydney, Sydney, NSW 2006, Australia

(Received 1 July 2011; revised 2 September 2011; accepted 12 October 2011; first published online 14 November 2011)

Granular materials segregate by size when sheared, which increases the destructive power in avalanches and causes demixing in industrial flows. Here we present a concise theory to describe this phenomenon for systems that for the first time include particles of arbitrary size. The evolution of the grainsize distribution during flow is described based on mass and momentum conservation. The theory is derived in a five-dimensional space, which besides position and time, includes a grainsize coordinate. By coupling the theory with a simple constitutive law we predict the kinematics of the flow, which depends on the grainsize dynamics. We show that the underpinning mechanism controlling segregation is a stress variation with grainsize. The theory, solved by a finite difference scheme, is found to predict the dynamics of segregation consistent with results obtained from discrete element simulations of polydisperse granular flow down inclined planes. Moreover, when applied to bimixtures, the general polydisperse theory reveals the role of grainsize contrast.

Key words: granular media, pattern formation, granular mixing

1. Introduction

One of the most distinct forms of pattern formation in granular materials is that observable in flows with particles of different size or density. As they flow the grains segregate, forming complex patterns. This is a concern for industrial applications where generally particles are required to be well mixed. Segregation occurs in flows down planes and in rotating cylinders, drums and blenders (Bridgwater 1976; Shinbrot, Alexander & Muzzio 1999; Ottino & Khakhar 2000), which are used for a variety of applications in the pharmaceutical, chemical, food, ceramic and construction industries. For a recent comprehensive review of the subject see Gray & Ancey (2011).

It has been noted for some time (Bridgwater & Ingram 1971; Savage & Lun 1988) that segregation down inclined planes occurs due to fluctuations in the local pores within the flow, a process termed ‘kinetic sieving’. With increasing shear strain rate, those fluctuations become more frequent. As new void spaces are created and grow, smaller particles are more likely to fit and fall into the pores. This results in a flux of small particles downwards through the bulk and a corresponding flux of large particles upwards. The segregation velocity, therefore is expected to increase with the rate of creation of voids, and therefore with the shear strain rate.

† Email address for correspondence: itai.einav@sydney.edu.au

Here we present a theory that describes this phenomenon for systems that for the first time include mixtures of arbitrary sizes. While this topic has been investigated for bimixtures (Savage & Lun 1988; Dolgunin, Kudy & Ukolov 1998; Gray & Thornton 2005; Gray & Chugunov 2006; May, Shearer & Daniels 2010), it has only recently been extended to 'multicomponent' systems (Gray & Ancey 2011), with n phases in the mixture. In that theory, particles are ranked from smallest to largest, without specifying the actual radii. Consequently, the number of free parameters increases quadratically with n, which are grouped into a single function that is not connected to the actual sizes. In the following section we introduce an alternative continuum theory that does include the actual sizes using a continuous grainsize coordinate. In § 4.4, we discuss the fundamental differences of the two approaches.

2. Continuum theory

We describe an avalanche of depth H, subjected to gravity g, where the largest particle has radius s_M and density ρ_0. The following theory is described non-dimensionally. Properties are non-dimensionalized as follows: length by H, grainsize by s_M, time by $\sqrt{H/g}$, velocity by $\sqrt{Hg}$ and stress by $\rho_0 g H$.

2.1. *A polydisperse mixture*

Mixtures are generally described by accounting for the various constituents and their interactions during flow, such as in Morland (1992). These constituents are commonly fluids, gases and solids, and a finite number of such constituents are treated simultaneously. Here, only solid phases in the flow are considered and we replace the finite number of constituents with a single grainsize coordinate that maps the grain radii continuously. This allows us to describe a mixture made of arbitrarily sized solids. To do this, we introduce a volumetric grainsize distribution $\phi(\boldsymbol{r}, s, t)$, of a particular grainsize s, at some location in space $\boldsymbol{r} = \{x, y, z\}$ and at time t:

$$\Phi[s_a < s < s_b] = \int_{s_a}^{s_b} \phi(s')\,\mathrm{d}s', \tag{2.1}$$

where Φ is the solid fraction of grains with grainsize above s_a and below s_b. Here ϕ then represents a probability density function for the grainsize distribution at every point in space and time, which satisfies

$$\int \phi\,\mathrm{d}s = 1, \quad \int \phi s\,\mathrm{d}s = \bar{s}, \tag{2.2}$$

where $\bar{s}(\boldsymbol{r}, t)$ is the average particle radius.

In the following, there is a distinction between intrinsic and partial properties. Intrinsic properties refer to a particular grainsize, whereas partial properties refer to the contribution of the intrinsic property of a particular grainsize to the average property.

2.2. *Density*

The intrinsic density, $\rho^*(s)$, is defined as the mass of a unit volume of particles with grainsize s. We allow particles belonging to a particular grainsize s to have different intrinsic density. Therefore, the partial density, $\rho(\boldsymbol{r}, s, t)$, and the bulk (or average) density, $\bar{\rho}(\boldsymbol{r}, t)$, are defined as

$$\rho = \phi\rho^*, \quad \bar{\rho} = \int \rho\,\mathrm{d}s. \tag{2.3}$$

2.3. *Stress*

Stresses are defined in a similar manner to the densities. Accordingly, the intrinsic stress, $\boldsymbol{\sigma}^*(\boldsymbol{r}, s, t)$, is the Cauchy stress on the solid part of a representative volume–grainsize element, meaning an element that refers not only to grains that belong to a certain volume in space, but also to a certain grainsize bin. This stress could be measured, for example using discrete element simulations, as detailed in § 3, where it will be shown to depend on the grainsize. For this reason, we require that the intrinsic stress varies with grainsize s in such a manner that

$$\boldsymbol{\sigma}^* = \bar{\boldsymbol{\sigma}} f, \quad \boldsymbol{\sigma} = \phi \boldsymbol{\sigma}^*, \quad \bar{\boldsymbol{\sigma}} = \int \boldsymbol{\sigma} \, \mathrm{d}s, \tag{2.4}$$

where the intrinsic stress scales about some average, or bulk stress $\bar{\boldsymbol{\sigma}}(\boldsymbol{r}, t)$ with scaling $f(\boldsymbol{r}, s, t)$. We also define the partial stress of each constituent, $\boldsymbol{\sigma}(\boldsymbol{r}, s, t)$. For (2.4) to hold, we require that

$$\int f \phi \, \mathrm{d}s = 1. \tag{2.5}$$

For a given size s, if $f < 1$ the intrinsic stress felt by that size is less than the bulk stress, and if $f > 1$ the intrinsic stress is greater than the bulk stress.

2.4. *Conservation of mass*

Following Ramkrishna (2000), we define a domain in the particle state space, $\Lambda(t)$, which contains a finite mass of particles which deforms over time. This domain can be split into two subdomains containing, first, the external physical space $\Lambda_{\boldsymbol{r}}$ and, second, the internal coordinate space Λ_s, where s is the grainsize coordinate. With the assumption that no particles enter or leave this domain, i.e. that there is no breakage or agglomeration, we may write in terms of the partial density ρ,

$$\frac{\mathrm{d}}{\mathrm{d}t} \int_{\Lambda_s(t)} \int_{\Lambda_{\boldsymbol{r}}(t)} \rho \, \mathrm{d}V_{\boldsymbol{r}} \, \mathrm{d}s = 0, \tag{2.6}$$

where $\mathrm{d}V_{\boldsymbol{r}}$ is an infinitesimal physical volume in real space and $\mathrm{d}s$ is the equivalent property in the grainsize direction. Using a generalization of Reynolds' transport theorem to general vector spaces,

$$\int_{\Lambda_s(t)} \int_{\Lambda_{\boldsymbol{r}}(t)} \left[\frac{\partial \rho}{\partial t} + \frac{\partial}{\partial s}(\rho \dot{S}) + \boldsymbol{\nabla}_{\boldsymbol{r}} \cdot (\rho \dot{\boldsymbol{R}}) \right] \mathrm{d}V_{\boldsymbol{r}} \, \mathrm{d}s = 0, \tag{2.7}$$

where $\dot{S}$ and $\dot{\boldsymbol{R}}$ are the instantaneous velocities of material ρ in the s and $\boldsymbol{r}$ directions, respectively, and $\boldsymbol{\nabla}_{\boldsymbol{r}} = \{\partial/\partial x, \partial/\partial y, \partial/\partial z\}$. Because the domain of these integrals is arbitrary, and the integral is continuous, we recover the population balance equation of the mass in a five-dimensional space $\{\boldsymbol{r}, s, t\}$

$$\frac{\partial \rho}{\partial t} + \frac{\partial}{\partial s}(\rho \dot{S}) + \boldsymbol{\nabla}_{\boldsymbol{r}} \cdot (\rho \dot{\boldsymbol{R}}) = 0. \tag{2.8}$$

We set $\dot{S} = 0$, which implies that particles do not grow or reduce over time. This is contrasted with Ricard & Bercovici (2009), who explored growth and reduction via diffusion in grainy materials, where the physical motion of constituents was not explored. We also make the following assumption

$$\rho \dot{\boldsymbol{R}} = \rho \boldsymbol{u} - D \boldsymbol{\nabla}_{\boldsymbol{r}} \rho, \tag{2.9}$$

so that the fluxes in physical space are split into two components due to the advective flux, $\rho \boldsymbol{u}$, where $\boldsymbol{u}(\boldsymbol{r}, s, t) = \{u, v, w\}$, and the diffusive flux, $D\boldsymbol{\nabla}_{\boldsymbol{r}}\rho$, with some constant diffusion coefficient D, which we will discuss further in § 3. We can then write

$$\frac{\partial \rho}{\partial t} + \boldsymbol{\nabla}_{\boldsymbol{r}} \cdot (\rho \boldsymbol{u}) = \boldsymbol{\nabla}_{\boldsymbol{r}} \cdot (D \boldsymbol{\nabla}_{\boldsymbol{r}} \rho). \tag{2.10}$$

Considering a flow that is uniform in the downslope (x) and cross-slope (y) directions, and segregating in the normal (z) direction, we retain a three-dimensional system in $\{z, s, t\}$, describing the evolution of the grainsize distribution ϕ via

$$\frac{\partial \rho}{\partial t} + \frac{\partial}{\partial z}(\rho w) = D \frac{\partial^2 \rho}{\partial z^2}, \tag{2.11}$$

where it is noted that both ρ and w depend on the grainsize coordinate.

2.5. *Conservation of momentum*

Conservation of momentum for our system can be expressed as

$$\frac{\mathrm{d}}{\mathrm{d}t} \int_{\Lambda_s(t)} \int_{\Lambda_{\boldsymbol{r}}(t)} \rho \dot{\boldsymbol{R}} \, \mathrm{d}V_{\boldsymbol{r}} \, \mathrm{d}s = \int_{\Lambda_s(t)} \int_{\Lambda_{\boldsymbol{r}}(t)} \phi \boldsymbol{F}^* \, \mathrm{d}V_{\boldsymbol{r}} \, \mathrm{d}s, \tag{2.12}$$

where $\boldsymbol{F}^*(\boldsymbol{r}, s, t)$ is the intrinsic force per representative volume–grainsize element. By again using Reynolds' transport theorem, and the arbitrariness of the intergrands,

$$\frac{\partial}{\partial t}(\rho \dot{\boldsymbol{R}}) + \boldsymbol{\nabla}_{\boldsymbol{r}} \cdot (\rho \dot{\boldsymbol{R}} \otimes \dot{\boldsymbol{R}}) = \phi \boldsymbol{F}^*, \tag{2.13}$$

where $\otimes$ is the outer product. The left-hand side of the equality represents the material derivative of partial density ρ. Adapting the expressions in Gray & Thornton (2005) and Gray & Chugunov (2006), we set $\boldsymbol{F}^*$ as

$$\boldsymbol{F}^* = -\boldsymbol{\nabla}_{\boldsymbol{r}} \cdot \boldsymbol{\sigma}^* + \rho^* \boldsymbol{g} - \frac{\bar{\rho} c}{\dot{\gamma}} (\boldsymbol{u} - \bar{\boldsymbol{u}}). \tag{2.14}$$

Note that unlike the work of Gray and colleagues, our definition of the partial force $\phi \boldsymbol{F}^*$ was specified in a way that allows the identification of an intrinsic force $\boldsymbol{F}^*$, as was done for density and stress (see § 2.1). Specifically, the first term on the right-hand side represents a force due to the gradient of intrinsic stress. The second term represents the intrinsic body force due to gravity $\boldsymbol{g}$. The final term arises from the interaction of each species with the bulk. Here $\bar{\boldsymbol{u}}(\boldsymbol{r}, t) = \int \phi \boldsymbol{u} \, \mathrm{d}s$ and c is a coefficient of interparticle drag, with units of inverse time, to allow normalization by the shear rate $\dot{\gamma}(\boldsymbol{r}, t)$. Subsequently, drag force reduces with increasing fluctuation in local pore creation. The exact nature of the parameter c is poorly understood and is therefore taken as constant. At least, it represents the effects of particle shape, surface roughness and concavity in terms of their effect on the size segregation velocity.

For simplicity, we assume that the flow is quasisteady, and that the acceleration terms $(\partial/\partial t)(\rho \dot{\boldsymbol{R}})$ and $\boldsymbol{\nabla}_{\boldsymbol{r}} \cdot (\rho \dot{\boldsymbol{R}} \otimes \dot{\boldsymbol{R}})$ can be neglected. This implies that $\boldsymbol{F}^* = 0$ with a weak form that can be expressed as $\int \int \phi \boldsymbol{F}^* \, \mathrm{d}V_{\boldsymbol{r}} \, \mathrm{d}s = 0$. From this and (2.2)–(2.5) we obtain

$$\boldsymbol{\nabla}_{\boldsymbol{r}} \cdot \bar{\boldsymbol{\sigma}} = \bar{\rho} g. \tag{2.15}$$

Considering a flow that is uniform in the downslope (x) and cross-slope (y) directions, and without stress at the free surface,

$$\bar{\sigma}_{xz} = \bar{\rho} g \sin\theta (1 - z), \quad \bar{\sigma}_{zz} = \bar{\rho} g \cos\theta (1 - z). \tag{2.16}$$

Then, after rearrangement, $\boldsymbol{F}^* = 0$ becomes

$$w(s) = \dot{\gamma}\frac{g\cos\theta}{c}\left(f - \frac{\rho^*}{\bar{\rho}}\right), \tag{2.17}$$

where we have used the fact that $\bar{w} = 0$. This tells us that particles will move relative to other sizes for two reasons. The first, and the most important for this study, is if they feel a partial stress which is different from their neighbours. The second is if they feel either a positive or negative buoyancy.

For plug flow, where $\dot{\gamma} = 0$, we expect no segregation to occur because the velocity is constant everywhere and local voids should not be created.

We can now combine our segregation velocity (2.17) with (2.11) to conclude that our governing population balance equation for grainsize distribution ϕ is

$$\frac{\partial\phi}{\partial t} + \frac{g\cos\theta}{c}\cdot\frac{\partial}{\partial z}\left(\phi\dot{\gamma}\left(f - \frac{\rho^*}{\bar{\rho}}\right)\right) = D\frac{\partial^2\phi}{\partial z^2}. \tag{2.18}$$

2.6. *Constitutive theory*

We use a simple constitutive equation that is known to be reasonable for steady, dense flowing granular media down inclines (MiDi 2004; da Cruz *et al.* 2005), as a first-order approximation in $\dot{\gamma}$

$$\frac{\bar{\sigma}_{xz}}{\bar{\sigma}_{zz}} = \mu_c + kt_i\dot{\gamma}, \tag{2.19}$$

where μ_c is the angle of repose of our material, k is a non-dimensional constant and t_i is the inertial time. For quasimonodisperse systems, the inertial time represents the typical time for a particle to move a distance of its own radius, driven by the normal stress. Rognon *et al.* (2007) suggested that for bidisperse flows such a behaviour is still valid provided that the inertial time involves the average size of the mixture, $\bar{s}$. Although the precise dependence of the rheology on the polydispersity is still a matter of research (Yohannes & Hill 2010), we shall here employ the simplest hypothesis for polydisperse mixtures. Following Rognon *et al.* (2007), we equate the force due to $\bar{\sigma}_{zz}$ with the inertial force on a particle of size $\bar{s}$ with density $\bar{\rho}$ and a typical acceleration $2\bar{s}/t_i^2$. This gives $4\pi\bar{s}^2\bar{\sigma}_{zz} = \bar{\rho}(4\pi\bar{s}^3/3)\cdot(2\bar{s}/t_i^2)$, from which the inertial time is $t_i = \bar{s}\sqrt{2\bar{\rho}/3\bar{\sigma}_{zz}}$. Considering the stress profile within a flow down a slope, (see (2.16)) the shear strain rate profile is

$$\dot{\gamma} = \frac{\tan\theta - \mu_c}{k\bar{s}}\sqrt{3/2g\cos\theta(1-z)}. \tag{2.20}$$

Because $\bar{s}$ varies with time, the shear strain rate does as well. This implies that segregating flows are non-steady, unlike our assumption employed to simplify the momentum conservation. Nevertheless, we will see in § 3 that this steadiness assumption is already very useful. Introducing this shear strain rate profile in (2.17) provides the segregation velocity as

$$w = \frac{C\sqrt{1-z}}{\bar{s}}\left(f - \frac{\rho^*}{\bar{\rho}}\right), \tag{2.21}$$

where $C = (((\tan\theta - \mu_c)g\cos\theta)/kc)\sqrt{(3/2)g\cos\theta}$.

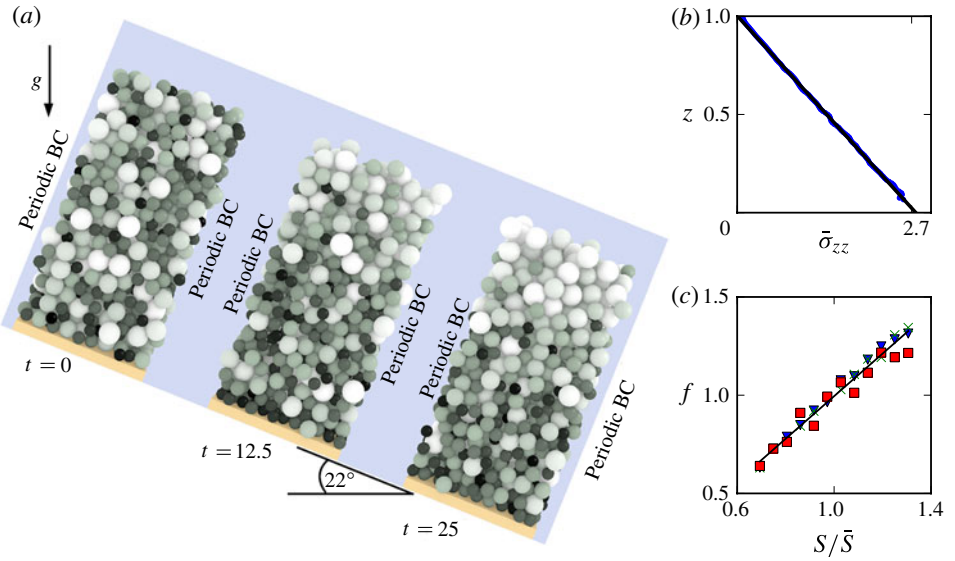

FIGURE 1. (Colour online available at journals.cambridge.org/flm) Size segregation in a polydisperse discrete element method (DEM) sample. (*a*) At $t = 0$, an initial sample of 1550 particles begins flowing downslope. By $t = 12.5$ the sample has begun to segregate by size, with larger particles collecting at the top of the flow, and smaller particles sinking to the base. By $t = 25$ the sample has reached its final segregated state. (*b*) Bulk vertical stress $\bar{\sigma}_{zz}$ is shown as a function of height, predicted by (2.16). (*c*) Size dependence of intrinsic stress expressed using the scaling function f. We split the simulation into three even layers by depth. The top ($\triangledown$), middle ($\times$) and bottom ($\square$) thirds are shown separately, yet all fit a linear scaling given by (3.1). For both right-hand plots, solid lines indicate linear fits to the data.

3. Discrete element method model

Looking at the population balance (2.18), we only require C, D and f to complete the system. However, this Section demonstrates that the latter two are measurable, leaving C as the only free parameter.

To measure f, we would like to know how the intrinsic stress $\boldsymbol{\sigma}^*$ scales with grainsize. To do this, we implemented a standard discrete element method (DEM) to simulate the flow down an inclined plane of a polydisperse mixture of spheres, with $s \in [0.5, 1]$ distributed uniformly by volume (see figure 1). As usual, spheres interact by elastic (Hertzian) contacts, with some normal dissipation achieved through a dashpot element with coefficient of restitution of 0.6 and tangential friction (coefficient of friction of 0.4). There are 1550 particles in the sample: about 15 large particle diameters deep, 6 wide and 6 long, with periodic boundary conditions in the x and y directions. All of the particles have the same density. The base is a smooth plane inclined at an angle of $\theta = 22°$. At lower angles, the flow stops; at higher angles, the flow accelerates with increasing diffusion. The plane has some rolling resistance, mimicking roughness, to avoid plug flow (the expression for rolling resistance used can be found in Rognon *et al.* 2010). The particles are initially set randomly with no contacts, which infers consolidation, and given initial down slope velocities near to their steady state speeds that are established from a preliminary simulation. Here $t = 0$ is defined when the consolidation has completed (typically at times $-0.2 < t < 0$). This initial condition was chosen to reach steady state rapidly, before significant segregation has occurred.

Since we are interested in polydisperse simulations, the numbers of particles within a given grainsize bin is very limited. Therefore, this process was repeated 15 times and the results were averaged across the simulations, in effect providing nearly 25 000 grains.

At a given time t, the intrinsic stress was measured by summing all contact forces $\boldsymbol{F}_c$ acting at contacts c that belonged to particles in depth bin z and grainsize bin s as $\boldsymbol{\sigma}^*(z, s) \approx (1/V)\sum_c \boldsymbol{F}_c \otimes \boldsymbol{r}_c$ where $\boldsymbol{r}_c$ is the centre-to-centre vector and V is the total volume of particles in that bin. The bin dimensions were selected as small as possible while ensuring sufficient particles in each bin ($\Delta z = 0.01$, $\Delta s = 0.02$).

The bulk normal stress was calculated as the volume weighted average of the intrinsic stresses from all bins s at a particular height. As shown in figure 1, it follows that the bulk normal stress scales as $\bar{\sigma}_{zz} \propto 1 - z$, which is consistent with the prediction of (2.16). Moreover, we can measure at different depths the ratio between the intrinsic normal stress carried by one species σ^*_{zz} and the bulk stress $\bar{\sigma}_{zz}$ of all species, to obtain the function f (see figure 1). It appears that f admits a simple linear scaling with the grainsize, which is consistent with the requirement discussed in § 2.3

$$f(\boldsymbol{r}, s, t) = \frac{s}{\bar{s}}. \tag{3.1}$$

A similar grainsize scaling has been observed during uniaxial compression by Einav (2007), which highlights its significance in polydisperse media.

We also measure the self-diffusion coefficient using the standard expression (see for example Campbell 1997): $D = \langle \Delta z^2 / 2\Delta t \rangle$ where Δz represents a change in position during an time increment $\Delta t = 0.01$. The angle brackets denote an average made over all of the grains, and over some time. While D may in fact be a function of both $\dot{\gamma}$ and s (Utter & Behringer 2004), for simplicity we only focus here on a constant mean value. In these simulations, we measure $D \approx 0.007$ (the physical diffusion coefficient non-dimensionalized by $\sqrt{H^3 g}$).

We can now rewrite (2.18) using (3.1) and (2.21) to give the governing population balance equation of polydisperse segregation down inclined planes:

$$\frac{\partial \phi}{\partial t} + C\frac{\partial}{\partial z}\left(\frac{\phi\sqrt{1-z}}{\bar{s}}\left(\frac{s}{\bar{s}} - \frac{\rho^*}{\bar{\rho}}\right)\right) = D\frac{\partial^2 \phi}{\partial z^2}. \tag{3.2}$$

Lastly, the only free parameter in our theory, C, was fitted such that the DEM simulation took the same physical time to reach steady state as the numerical solution of the continuum theory. The theory can now be implemented in a finite element code, because it contains a constitutive model, albeit a simple one. This could also be solved in five-dimensional $\{\boldsymbol{r}, s, t\}$-space without the quasisteady assumption, using a more elaborate constitutive model, defined in tensorial form rather than the scalar form employed in this paper.

4. Results

4.1. *Solution of governing equation*

Solving the governing equation (3.2) is done numerically using a finite difference method. Simple methods for solving this class of equation are known to exhibit large amounts of numerical dissipation (LeVeque 2002). For that purpose we use a slope-limited total variation diminishing upstream-centred scheme (Quarteroni & Valli 1997) to approximate the numerical solution of the general equation in $\{z, s, t\}$.

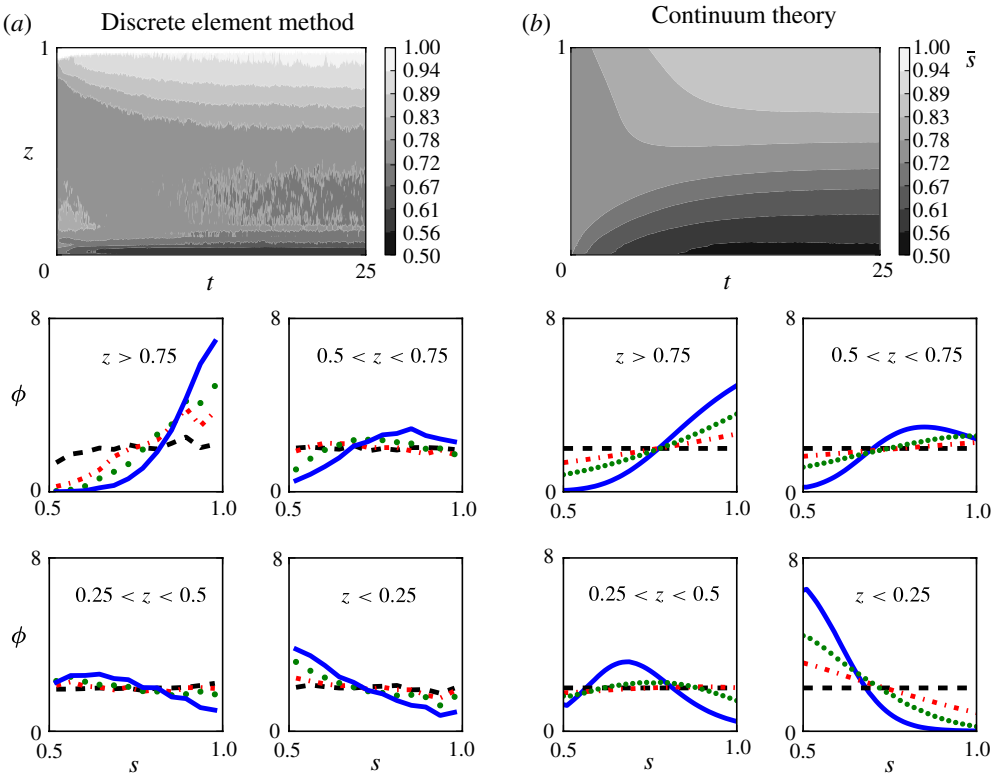

FIGURE 2. (Colour online) The DEM system (a) compared with an equivalent solution of the continuum theory. (b) Top: spatiotemporal plot of the average grainsize. Remaining: grainsize distributions at $t = 0$ (dashed), $t = 2$ (dash-dotted), $t = 5$ (dotted) and $t = 25$ (solid) averaged over different heights of the flow.

The system of equations is solved by discretizing along the z and s directions into a regularly spaced mesh, and a discretized set of grainsize distribution values $\phi^k_{i,j}$ is defined at each height i, grainsize j and time k. The mesh is defined so that the edges between cells lie at the midpoints $i \pm 1/2$. Across these edges the total flux is the sum of the fluxes due to the diffusive term $(\phi^k_{i,j} w^k_{i,j})$ and the advective term $(-D(\partial \phi^k_{i,j}/\partial z))$ in (3.2). A SuperBee flux limiter is used to minimize dissipation near discontinuities in the solution, and the resultant numerical flux, h, is constructed from upwinded left and right going fluxes for each $\phi^k_{i\pm 1/2,j}$ and then projected onto the solution at $\phi^{k+1}_{i,j}$. This can be summarized as

$$\phi^{k+1}_{i,j} = \phi^k_{i,j} - \frac{\Delta t}{\Delta z}(h^k_{i+1/2,j} - h^k_{i-1/2,j}), \tag{4.1}$$

and the whole scheme can be found in Quarteroni & Valli (1997, pp. 475–481). The solution for all grainsizes are coupled through the dependence of h on $\bar{s}$ and $\bar{\rho}$, which are updated each time step by summing over the n discrete grainsizes as $\bar{s}^k_i = \Delta s \sum_{j=1}^{n} \phi^k_{i,j} s_j$. Lastly, we impose a no flux boundary condition

$$C \frac{\phi \sqrt{1-z}}{\bar{s}} \left(\frac{s}{\bar{s}} - \frac{\rho^*}{\bar{\rho}} \right) = D \frac{\partial \phi}{\partial z} \quad \text{on } z = 0, 1. \tag{4.2}$$

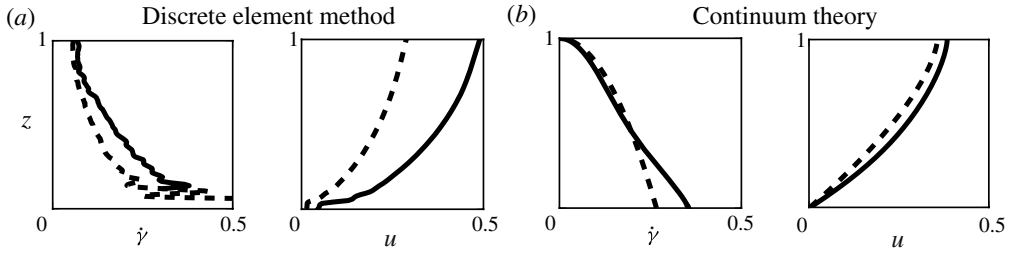

FIGURE 3. The DEM system (*a*) compared with an equivalent solution of the continuum theory. (*b*) For each system, the initial (dashed) and final (solid) shear strain rate and downslope velocity profiles are shown.

For the results shown here, we have used $\Delta s = \Delta z = 0.05$ and $\Delta t < \Delta z^2$. This numerical method has been used extensively for similar problems, such as in Gray & Thornton (2005), and has been shown to be stable and accurate, with a minimal amount of numerical dissipation.

4.2. *Results from polydisperse system*

On the left of figures 2 and 3 we represent the time evolution of the DEM sample shown in figure 1, and the equivalent solution of the analytic theory on the right. For that purpose, the theoretical model was solved with the values $D = 0.007$ (measured directly from the DEM in § 3) and $C = 0.2$ (to match the segregation time).

The theory predicts the grainsize distribution $\phi(s)$ at any time of the flow, here shown for four times, ranging from the initial to final stages. It is clear from both analyses that there is significant segregation, which feeds back in a way that intensifies the downslope velocity. Also, it appears that at steady state, diffusion prohibits stratification into layers of uniform grainsizes. Instead, the grainsize distribution has a non-trivial shape that varies with time and position. Nevertheless, the theory predicts qualitative agreement with the DEM realization.

In figure 3, the predictions of the continuum theory for $\dot{\gamma}$ and u are compared with the DEM, which shows comparable shear strain rate next to the basal plane, with both decaying strongly towards the free surface. The curvature of the strain rate profile is different. However, this discrepancy is likely related to the linear approximation of the constitutive law for dry granular flow (2.19). This is also known to be affected by the proximity of the plane (see for instance Rognon *et al.* 2007).

4.3. *Reduction to bimixture theory*

There are many theories describing kinetic sieving in bimixtures. The first such theory was that of Savage & Lun (1988), where statistical mechanics was employed to model the segregation. Later, Dolgunin & Ukolov (1995) and Gray & Thornton (2005) developed continuum models for non-diffusive flow by considering a bimixture with shared solid fraction between the two phases in the flow. More recently, Gray & Chugunov (2006) added diffusion to the previous continuum theories.

For the case of bimixtures, which involve only two distinct grainsizes, with the same intrinsic density, the grainsize distribution ϕ can be represented as a polydisperse mixture with the help of two dirac δ-functions. For two grainsizes $s = \{s_a, s_b\}$ the bidisperse case takes the following grainsize distribution

$$\phi = \Phi_a \delta(s - s_a) + \Phi_b \delta(s - s_b), \quad \Phi_a + \Phi_b = 1, \tag{4.3}$$

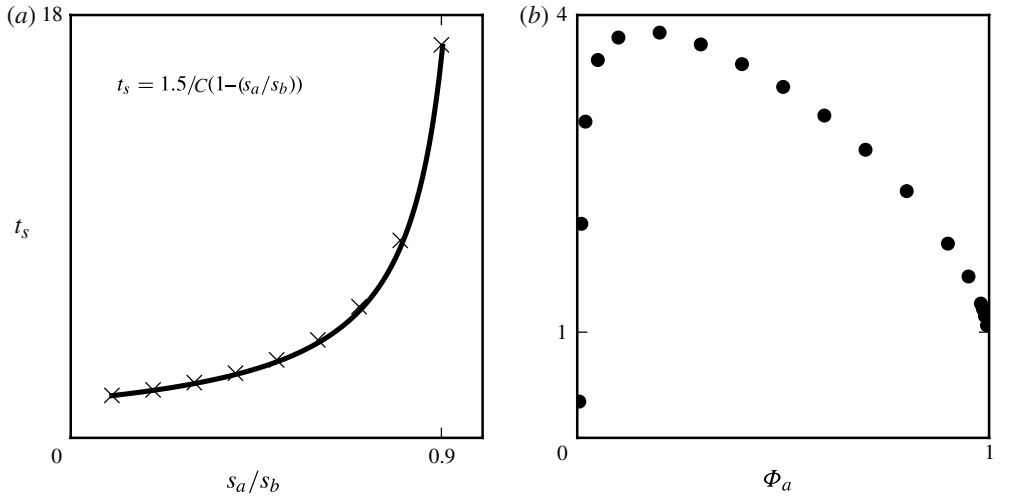

FIGURE 4. The time for complete segregation in bidisperse systems. (*a*) The time as a function of small grainsize s_a, with $s_b = 1$ and $\Phi_a = 0.5$. The solid line indicates a hyperbolic trend for the segregation time. (*b*) The time for complete segregation as a function of small particle concentration, Φ_a, for two grainsizes $s_a = 0.5$ and $s_b = 1$.

where Φ_a and Φ_b are the solid fractions of the two species. For this case, using (2.17) and (3.1), the segregation velocity of the large particles ($s = s_b$) becomes

$$w(s_b) = \dot{\gamma} \left(\frac{g \cos\theta}{c} \right) \left(\frac{s_b - s_a}{\bar{s}} \right) (1 - \Phi_b), \tag{4.4}$$

where $\bar{s} = s_a \Phi_a + s_b \Phi_b$. Compare this with equation (3.11) of Gray & Thornton (2005): $w^b = ((Bg \cos\theta)/c)(1 - \Phi_b)$, where B/c controls the rate of segregation in their model. As in May *et al.* (2010), our formulation explicitly represents the role of the shear rate. Unlike the previous works of Gray & Thornton (2005) and May *et al.* (2010), we capture the effects of grainsize difference and the time-dependent local average grainsize.

Experiments by Wiederseiner *et al.* (2011) have shown good agreement with the theory presented by Gray & Chugunov (2006) for one set of particle sizes ($s_a = 1$ mm, $s_b = 2$ mm). Using this new formulation, it is now possible to explore the sensitivity of such systems to alternative grainsizes.

We use $\int_0^1 \int_0^1 |\partial\phi/\partial t| \, \mathrm{d}z \, \mathrm{d}s \leqslant 0.01$ as a criterion for a steady-state solution, applied for the case of $D = 0$. Using this definition, in figure 4 we represent this segregation time, t_s, as a function of initial conditions for a variety of bimixtures. On the left, increasing the size contrast between the particle species reduces the time for segregation. On the right, for a mixture with grainsize ratio of two, and $C = 1$, there is a maximum in the time for segregation at a concentration of approximately 20 % small particles. These results await experimental validation. However, an explanation for this has already been proposed using a simple cellular automaton, as being due to the asymmetry of the shear strain rate (Marks & Einav 2011).

4.4. *Reduction to multicomponent theory*

Recently, Gray & Ancey (2011) proposed a multicomponent theory which extends the work presented in Gray & Thornton (2005) to many dirac δ-functions. For this case,

which involves a discrete number of grainsizes, n, with the same intrinsic density, the grainsize distribution ϕ can be represented as a sum of dirac δ-functions. For grainsizes $i = \{1, 2, \ldots, n\}$ the multicomponent case takes the following grainsize distribution

$$\phi = \sum_{i=1}^{n} \Phi_i \delta(s - s_i), \quad \sum_{i=1}^{n} \Phi_i = 1, \quad \bar{s} = \sum_{i=1}^{n} \Phi_i s_i, \tag{4.5}$$

where Φ_i is the solid fraction of species i, and each i is chosen to perfectly tessellate the grainsize distribution. For this case, using (2.17) and (3.1), the segregation velocity of grainsize s_i becomes

$$w(s_i) = \dot{\gamma} \left(\frac{g \cos\theta}{c} \right) \left(\frac{s_i}{\sum_{i=1}^{n} \Phi_i s_i} - 1 \right), \tag{4.6}$$

which is not immediately comparable to the result produced by Gray & Ancey (2011). As a means of drawing a reasonable comparison, let us specify a geometrical sequence for the discrete size bins, such as the jth bin being twice the size of the $(j-1)$th bin, or $s_j = s_0 \cdot 2^j$, for some smallest size s_0. This set of bin sizes was found to be useful for defining grading entropy (Lorincz *et al.* 2005). Equation (4.6) then becomes

$$w(s_i) = \dot{\gamma} \left(\frac{g \cos\theta}{c} \right) \sum_{j=1}^{n} B_{ij} \Phi_j, \tag{4.7}$$

where $B_{ij} = (1 - 2^{j-i})/(\sum_{m=1}^{n} \Phi_m 2^{m-i})$. Similarly, distributing the grainsize bins linearly, $s_j = s_0 + \Delta s \cdot j$, gives $B_{ij} = (i - j)/(\sum_{m=1}^{n} \Phi_m((s_0/\Delta s) + m))$. Compare these with equations (2.22)–(2.23) of Gray & Ancey (2011), with no diffusion ($D_r = 0$) where $w_i = ((g \cos\theta)/c) \sum_{j=1}^{n} B_{ij} \Phi_j$. Gray & Ancey (2011) introduced $(1/2)n(n-1)$ constants B_{ij}, as a means to construct analytic solutions. According to our theory these coefficients are not constant, but vary with time through Φ_m. Furthermore, they also depend on the allocation of the grainsize bins, which is now obtained naturally by associating each w_i with a grainsize s_i, without requiring additional parameters.

5. Conclusions

In this paper we have derived a polydisperse theory for granular segregation, where we have introduced the notion of a grainsize coordinate. The result of this is a five-dimensional population balance equation. By specifying this for inclined plane flows, this equation simplifies to three dimensions. Pivotal to our theory is the description of intrinsic stresses that scale with grainsize and control the segregation dynamics. The use of a simple constitutive equation that relates the shear stress and the shear strain rate enables us to connect the kinematics to the variation of grainsize distribution. We predict a grainsize distribution and a shear strain rate at any time and at any point in space.

Using this theory we have been able to model the segregation in systems of arbitrary grainsize distributions. Numerical solutions of the resulting nonlinear population balance equation are solved using a finite difference scheme. Comparison has been made with DEM simulations and consistent results have been found.

By employing our polydisperse theory to describe segregation in a bidisperse system, we have been able to compare our formulation with previous predictions (Gray & Thornton 2005). In this bidisperse limit, we now understand the role of size contrast between the constituents, and how that affects both the time for segregation, and the kinematics of the flow. We have also shown how multicomponent systems can be expressed in terms of the polydisperse theory, and how the fitting parameters used vary with time and with the choice of grainsize bins.

It is now possible to predict the time for segregation in geophysical and industrial flows and then to tailor conditions to either reduce or increase the extent of segregation as necessary. This has relevance for industrial applications that use granular materials, such as pharmaceutics, agriculture and mining. This can also increase our understanding of long run out landslides, since we predict a shear strain rate profile, and hence a downslope velocity profile. Also, these dynamics, with the added ingredient of momentum conservation, could be used for the design of protection structures.

Acknowledgements

We would like to thank the members of the Particles and Grains Laboratory at The University of Sydney. I.E. acknowledges grant DP0986876 from the ARC.

REFERENCES

BRIDGWATER, J. 1976 Fundamental powder mixing mechanisms. *Powder Technol.* **15** (2), 215–236.

BRIDGWATER, J. & INGRAM, N. D. 1971 Rate of spontaneous inter-particle percolation. *Chem. Engng Res. Des.* **49a**, 163–169.

CAMPBELL, C. S. 1997 Self-diffusion in granular shear flows. *J. Fluid Mech.* **348**, 85–101.

DA CRUZ, F., EMAM, S., PROCHNOW, M., ROUX, J-N. & CHEVOIR, F. 2005 Rheophysics of dense granular materials: discrete simulation of plane shear flows. *Phys. Rev.* E **72**, 021309.

DOLGUNIN, V. N. & UKOLOV, A. A. 1995 Segregation modelling of particle rapid gravity flow. *Powder Technol.* **83** (2), 95–104.

DOLGUNIN, V. N., KUDY, A. N. & UKOLOV, A. A. 1998 Development of the model of segregation of particles undergoing granular flow down an inclined chute. *Powder Technol.* **96** (3), 211–218.

EINAV, I. 2007 Breakage mechanics – part 1: theory. *J. Mech. Phys. Solids* **55** (6), 1274–1297.

GRAY, J. M. N. T. & ANCEY, C. 2011 Multi-component particle-size segregation in shallow granular avalanches. *J. Fluid Mech.* **678**, 535–588.

GRAY, J. M. N. T. & CHUGUNOV, V. A. 2006 Particle-size segregation and diffusive remixing in shallow granular avalanches. *J. Fluid Mech.* **569**, 365–398.

GRAY, J. M. N. T. & THORNTON, A. R. 2005 A theory for particle size segregation in shallow granular free-surface flows. *Proc. R. Soc.* A **461** (2057), 1447–1473.

LEVEQUE, R. J. 2002 *Finite Volume Methods for Hyperbolic Problems*. Cambridge University Press.

LORINCZ, J., IMRE, E., GLOS, M., TRANG, Q. P., RAJKAI, K., FITYUS, S. & TELEKES, G. 2005 Grading entropy variation due to soil crushing. *Intl J. Geomech.* **5** (4), 311–319.

MARKS, B. & EINAV, I. 2011 A cellular automaton for segregation during granular avalanches. *Granul. Matt.* **13**, 211–214.

MAY, L. B. H., SHEARER, M. & DANIELS, K. E. 2010 Scalar conservation laws with non-constant coefficients with application to particle size segregation in granular flow. *J. Nonlinear Sci.* 1–19.

MIDI, G. D. R. 2004 On dense granular flows. *Eur. Phys. J.* E **14** (4), 341–365.

MORLAND, L. 1992 Flow of viscous fluids through a porous deformable matrix. *Surv. Geophys.* **13** (3), 209–268.

OTTINO, J. M. & KHAKHAR, D. V. 2000 Mixing and segregation of granular materials. *Annu. Rev. Fluid Mech.* **32** (1), 55–91.

QUARTERONI, A. & VALLI, A. 1997 *Numerical Approximation of Partial Differential Equations*. Springer.

RAMKRISHNA, D. 2000 *Population Balances: Theory and Applications to Particulate Systems in Engineering*. Academic.

RICARD, Y. & BERCOVICI, D. 2009 A continuum theory of grain size evolution and damage. *J. Geophys. Res. (Solid Earth)* **114** (13), 01204.

ROGNON, P., EINAV, I., BONIVIN, J. & MILLER, T. 2010 A scaling law for heat conductivity in sheared granular materials. *EPL* **89** (5), 58006.

ROGNON, P. G., ROUX, J. N., NAAÏM, M. & CHEVOIR, F. 2007 Dense flows of bidisperse assemblies of disks down an inclined plane. *Phys. Fluids* **19**, 058101.

SAVAGE, S. B. & LUN, C. K. K. 1988 Particle size segregation in inclined chute flow of dry cohesionless granular solids. *J. Fluid Mech.* **189**, 311–335.

SHINBROT, T., ALEXANDER, A. & MUZZIO, F. J. 1999 Spontaneous chaotic granular mixing. *Nature* **397**, 675–678.

UTTER, B. & BEHRINGER, R. P. 2004 Self-diffusion in dense granular shear flows. *Phys. Rev.* E **69** (3), 031308.

WIEDERSEINER, S., ANDREINI, N., ÉPELY-CHAUVIN, G., MOSER, G., MONNEREAU, M., GRAY, J. M. N. T. & ANCEY, C. 2011 Experimental investigation into segregating granular flows down chutes. *Phys. Fluids* **23** (1), 013301.

YOHANNES, B. & HILL, K. M. 2010 Rheology of dense granular mixtures: particle-size distributions, boundary conditions, and collisional time scales. *Phys. Rev.* E **82** (6), 061301.